THE JOURNAL OF PHYSICAL CHEMISTRY A

© Copyright 2007 by the American Chemical Society VOLUME 111, NUMBER 2, JANUARY 18, 2007

ARTICLES

Effects of Proximity on the Relaxation Dynamics of Flindersine and 6(5*H*)-Phenanthridinone

Pier Luigi Gentili, Fausto Ortica, Aldo Romani, and Gianna Favaro*

Dipartimento di Chimica, Università di Perugia, 06123 Perugia, Italy

Received: July 21, 2006; In Final Form: November 2, 2006

The role played by the carbonyl group in the antenna system of a naturally occurring photochromic chromene, flindersine (FL), has been experimentally investigated and compared with that of a carbonyl group present in a structurally related unreactive heterocyclic compound, 6(5*H*)-phenanthridinone (PH). Through stationary and time-resolved absorption and emission techniques, the excited-state relaxation dynamics after UV irradiation were determined for FL and PH. The presence of a carbonyl group in both compounds entails the existence of two close-lying, strongly coupled electronic excited states, having n,π^* and π,π^* character, respectively. Their coupling can be modulated by a careful choice of the solvent proticity and temperature. Moreover, in the case of strong coupling between the n,π^* and π,π^* states, we have proved that the relaxation dynamics can involve transitions in which the upper of the coupled states acts as an intermediate for radiationless decay, bypassing the lowest emissive state, whereby the fluorescence quantum yield becomes a function of the excitation wavelength.

Introduction

Aromatic carbonyl and nitrogen-heterocyclic compounds often exhibit luminescence that is strongly dependent on temperature, chemical substitution, and hydrogen-bonding power of the solvent.[1] This phenomenology can be traced to the close proximity of n,π^* and π,π^* electronic excited states, whereby it has been termed "proximity effect". Closely spaced n,π^* and π,π^* states can couple through out-of-plane bending modes and their coupling can lead to efficient radiationless decay to the ground state (S_0). Two theoretical formulations have been proposed for interpreting the influence of the n,π^* and π,π^* vibronic coupling on radiationless transitions, whose rate constant is expressed in the Golden-rule form. The first, by Lim et al.,[1] operates within the Frank−Condon principle. It entails that vibrational coordinate dependence of the adiabatic electronic wave function is neglected by invoking the Condon approximation, so that the vibronically active mode enters the matrix element of the radiationless transition only via the Franck−Condon factor. The second, by Siebrand and Zgierski,[2] deals with a non-Condon mechanism that incorporates the dependence of the adiabatic electronic wave function on the coordinates of the vibronically active modes. This dependence indirectly affects the matrix element of the radiationless transition from the lowest excited state induced by another nontotally symmetric mode.

In this work, we present and discuss experimental data regarding the proximity effect of a naturally occurring compound, flindersine, and a structurally related heterocyclic compound, 6(5*H*)-phenanthridinone (see Chart 1 for the structures of the two molecules).

Flindersine is a secondary metabolite produced by some plants, belonging to the family of Rutaceae[3] like *Flindersia Australis*. It belongs to the class of chromenes, and, as other chromenes synthesized by different plants, exhibits fungicidal and antimicrobial activity.[4]

* Address correspondence to this author. Phone: +39 075 5855573. Fax: +39 075 5855598. E-mail: favaro@unipg.it.

10.1021/jp0646426 CCC: $37.00 © 2007 American Chemical Society
Published on Web 12/14/2006

CHART 1

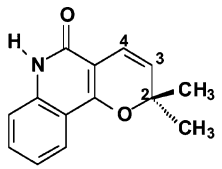

(I) Flindersine (FL)

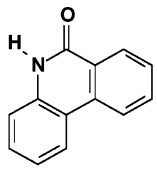

(II) 6(5*H*)-phenanthridinone (PH)

Chromenes are photochromic compounds[5] which in the dark exist in the closed, uncolored form, represented as **I** in Chart 1 for flindersine. The two π-electrons at the double bond C_3═C_4, electronically conjugated with a more or less extended π-electronic aromatic system (that in flindersine consists of a naphthalenic framework along with the amide group), and the couple of electrons located in the O_1 n-orbital (perpendicular to the molecular plane) constitute an antenna system harvesting UV radiation.[6] The energy of the absorbed electromagnetic radiation brings about a skeletal stretching of the π-system coupled to a ring puckering of the pyran moiety. The C_2-O_1 bond becomes more parallel to the extended π-system, whereby C_2-O_1 bond expansion is triggered, ultimately leading to its breakage. A final open colored structure is produced, which is metastable and can be transformed back to the original one, thermally and/or photochemically.

Several chromenes experimentally investigated so far[6−10] exhibited excitation wavelength-dependent photobehavior. This indicates that the electrocyclization reaction must occur on a barrierless excited-state surface and is so fast[11] to kinetically compete with unreactive relaxation processes, like intramolecular vibrational relaxation and intermolecular energy transfer.

The purpose of this work is to elucidate the role of the amide group in the antenna system of flindersine: the presence of a carbonyl group entails the existence of two close-lying n,π* and π,π* electronic excited states, presumably playing key roles in the relaxation dynamics of the molecule after excitation. The photoresponsive behavior of 6(5*H*)-phenanthridinone has been investigated as a matter of comparison. In our view, the results here presented constitute an experimental proof of the theoretical model, proposed by Siebrand and Zgierski,[2] predicting, in the case of strong coupling conditions between closely spaced excited states, higher order contributions to radiationless decay, namely, transitions in which the upper of the two coupled states acts as an intermediate.

Experimental Section

Materials. Flindersine (from John Morgan, Forest Products Research Laboratory, England) was used without further purification. 6(5*H*)-Phenanthridinone, purchased from Aldrich, was purified through HPLC. The solvent, 3-methylpentane (3MP), a reagent-grade Carlo Erba product, was distilled before use, whereas acetonitrile, ethanol, trifluoroethanol (all from Fluka), and *n*-hexane (Carlo Erba) were used as received. Water was deionized. Other compounds used as standards and energy donors or acceptors were anthracene (Baker) and β-carotene (Fluka), which were used as received, biacetyl (Aldrich), which was distilled, and thioxanthone (Baker), acridine (Fluka), and phenanthridine (K&K Laboratories), which were purified through HPLC. The 2,2′-dithienylketone was synthesized and purified for a previous work.[12]

Apparatus and Methods. *Steady State Absorption Measurements*. The absorption spectra at room temperature were recorded on a Perkin-Elmer Lambda 800 spectrophotometer or a Perkin-Elmer Lambda 5 spectrophotometer. A Hewlett-Packard 8453 diode array spectrophotometer was also used.

For the temperature control, a cryostat (Oxford Instruments), equipped with a temperature controller operating between 77 (if liquid nitrogen was adopted for cooling) and 500 K, was used. The temperature precision was within ±1 K; the accuracy in the temperature control was on the order of ±0.2 K.

The reaction quantum yield for flindersine was determined in the 230−80 K temperature range, by exciting at 321 nm. A 125 W Xe lamp, filtered by a Jobin-Yvon H10 monochromator (16 nm band-pass) and focused on the sample (in a fluorimetric 1 cm path cell) by a silica fiber optic, was used as an irradiating source. The irradiation was carried out at a right angle with respect to the monitoring beam of the spectrophotometer. The radiation intensity was determined by using potassium ferrioxalate actinometry. The emitted photon density was on the order of 5×10^{-7} mol of photons dm^{-3} s^{-1} at the irradiation wavelength. The flindersine concentration was on the order of 5×10^{-5} mol dm^{-3}.

Emission Measurements. Corrected emission spectra were recorded with a Spex Fluorolog-2 1680/1 spectrofluorimeter, controlled by the Spex DM 3000F spectroscopy software. To measure fluorescence quantum yields, Φ_F, corrected areas of the standard (anthracene in ethanol, $A = 0.05$ at 366 nm, calibrated with an absolute method[13]) and sample emissions were compared and corrected for the refraction index of the medium. The temperature effect on the refraction index was evaluated by using the following semiempirical relationship: $n(T_2) = n(T_1) + c \times \alpha\ (T_2 - T_1)$, where c and α are solvent constants.[14]

The fluorescence lifetimes were measured with both an Edinburgh Instruments 199S spectrofluorometer (using the single photon counting method with H_2 or a LED centered at 370 nm as sources, time resolution ca. 200 ps) and a Spex Fluorolog-τ2 system (using the phase modulation technique, time resolution ca. 30 ps).

The intersystem crossing quantum yield of 6(5*H*)-phenanthridinone in ethanol was determined at room temperature by measurements of biacetyl sensitized phosphorescence, using the appropriate Stern−Volmer equation and taking 2,2′-dithienylketone, which does not abstract hydrogen from the solvent, as a reference molecule, having $\Phi_T = 1$.[12] Data from quenching and sensitization measurements were corrected for trivial absorption by the quenchers of the exciting and emitted light. Excitation and emission wavelengths were selected to minimize the corrections.

Nanosecond Laser Flash Photolysis Measurements. For time-resolved laser flash photolysis measurements on the nanosecond time scale, the third harmonic ($\lambda_{exc} = 355$ nm) from a Continuum Surelite Nd:YAG laser was used with the energy less than 5 mJ per pulse and about 10 ns time resolution. Q-switch delays were used to reduce the laser intensity. Spectrophotometric analysis was performed by using a 150 W xenon source, a Baird-Tatlock monochromator blazed at 500 nm, a Hamamatsu R928 photomultiplier, and a Tektronix DSA 602 digital analyzer. The data were processed by a Tektronix PEP 301 computer.

For the measurements on 6(5*H*)-phenanthridinone, which absorbs at shorter wavelengths, the fourth harmonic ($\lambda_{exc} = 266$ nm) from the Nd:YAG laser was used.

The product $\Phi_T \times \epsilon_T$ (where Φ_T and ϵ_T are the triplet quantum yield and molar absorbance coefficient, respectively) was determined by calibrating the experimental setup with optically matched solutions of benzophenone in benzene ($\Phi_T \times \epsilon_T = 7200$ dm^3 mol^{-1} cm^{-1} at 520 nm) or in acetonitrile ($\Phi_T \times \epsilon_T = 6500$ dm^3 mol^{-1} cm^{-1} at 520 nm).[15] The molar

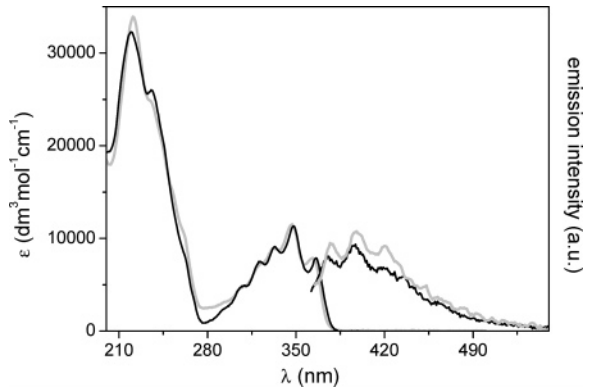

Figure 1. Absorption and fluorescence spectra of FL in 3MP (black) and ethanol (gray), recorded at room temperature.

absorbance coefficient of 6(5*H*)-phenanthridinone triplet in CH_3CN was determined through a sensitization method[16] by using benzophenone as a sensitizer ($\epsilon_T = 6500$ dm^3 mol^{-1} cm^{-1}, $\Phi_T = 1$, and $E_T = 288$ kJ mol^{-1})[15] because of its favorable spectral situation. Determining ϵ_T for 6(5*H*)-phenanthridinone in hydrocarbon solvents was impossible, since its extremely low solubility made unreliable recording any significant signal.

The triplet quantum yield of flindersine in benzene was measured by comparing the changes of absorbance of β-carotene triplet, sensitized by energy transfer from the substrate, and that sensitized by benzophenone, used as a standard ($\Phi_T = 1$), under the same experimental conditions (absorbance at 355 nm and β-carotene concentration). More details about the method of triplet quantum yield determinations are reported in the literature.[17]

Results

Flindersine (FL). It was previously reported[8] that the fluorescence (Φ_F) and reaction (Φ_{PC}) quantum yields of FL are functions of the vibronic level excited within a given progression of the first electronic excited state. In other words, FL exhibits "vibronic effects" in photochemistry and photophysics as well.

Figure 1 depicts the room temperature absorption and the emission spectra of FL in 3MP and EtOH. The absorption spectrum consists of two main electronic bands: the magnitude of the molar absorbance coefficients (10^4 dm^3 mol^{-1} cm^{-1}) suggests that they are generated by allowed electronic transitions. The band located at lower energy is vibronically structured with an energy difference between adjacent peaks of roughly 1300 cm^{-1}. The same fine structure appears in the emission band, centered at 395 nm. According to a simulation of absorption spectrum, based on the ZINDO/S (10×10) method, applied on a molecular geometry optimized for the ground state by the PM3 method, the band at lower energy is due to the HOMO−LUMO transition (predicted to be at 349 nm) having π,π^* character and involving the entire antenna system of FL. The antenna, harvesting UV radiation, is an extended electronic system including the n orbital on the oxygen atom of the pyran ring, perpendicular to the molecular plane, and the π electrons of the C_3═C_4 bond along with the two adjacent rings. The presence of the carbonyl group entails the existence of a (n,π^*) state, predicted by ZINDO/S calculation to give rise to a spectrally silent transition at 332 nm.

In Table 1, Stokes shifts ($\Delta\bar{\nu}$) and values of absolute fluorescence quantum yields (Φ_F) for FL in different solvents are reported. They are appreciably sensitive to the nature of the solvent. Increasing polarity, and/or hydrogen bonding ability of the solvent, leads to an increase in Φ_F and $\Delta\bar{\nu}$. For example,

TABLE 1: Stokes Shift and Fluorescence Quantum Yield (Φ_F) Determined for Flindersine in Various Solvents at Room Temperature in the Presence of Oxygen

solvent	stokes shift/$\Delta\bar{\nu}$ (cm^{-1})	Φ_F ($\lambda_{exc} = 321$ nm)
3MP	726	0.0007
n-hexane	726	0.0007
CH_3CN	826	0.0010
EtOH	952	0.0019
CF_3CH_2OH	1613	0.0027[a]

[a] Φ_F determined at $\lambda_{exc} = 327$ nm.

TABLE 2: Singlet Excited-State Parameters, Fluorescence Lifetime, and Radiative and Nonradiative Kinetic Constants for FL in Trimethylpentane, Ethanol, and Trifluoroethanol

solvent	*T*/K	τ_F/ns	k_F/s^{-1}	$\sum k_{nr}$/s^{-1}
3MP	78	1.42 ± 0.02	4×10^7	6.6×10^8
	298	≈0.1	$\approx 0.7 \times 10^7$	$\approx 1 \times 10^{10}$
EtOH	298	≈0.15	1.3×10^7	7×10^9
CF_3CH_2OH	298	≈0.2	1.3×10^7	5×10^9

passing from the nonpolar 3MP to the highly hydrogen-bonding trifluoroethanol, Φ_F increases almost 4 times and the Stokes shift is more than doubled. Furthermore, the Φ_F value in a specific solvent depends not only on the degree of vibronic excitation within the same electronic transition,[8] but also on the electronic state that is excited. In fact, by irradiating FL at $\lambda < 270$ nm, the fluorescence intensity was so weak to make impossible estimating Φ_F in every solvent except trifluoroethanol, where Φ_F ($\lambda_{exc} = 240$ nm) = 0.001 (i.e., less than a half of Φ_F at $\lambda_{exc} = 327$ nm).

The fluorescence quantum yield of FL is also significantly sensitive toward temperature. An 80-fold increase in Φ_F was observed between room temperature ($\Phi_F = 0.0007$) and 78 K ($\Phi_F = 0.0552$) in 3MP; in ethanol, Φ_F increased 20 times from 333 ($\Phi_F = 0.0006$) to 173 K ($\Phi_F = 0.0132$) and 4 times from 328 ($\Phi_F = 0.0017$) to 245 K ($\Phi_F = 0.0068$) in trifluoroethanol.

In Table 2, the kinetic parameters which characterize the singlet excited-state relaxation of FL are reported in three solvents. The radiative kinetic constant was calculated from the experimental fluorescence lifetime and quantum yield, $k_F = \Phi_F/\tau_F$, and the sum of all radiationless rate constants was determined as the difference, $\sum k_{nr} = 1/\tau_F - k_F$. In 3MP, by comparing the parameters at room temperature and 78 K, it can be noticed that the radiative rate constant was scarcely temperature dependent, whereas the $\sum k_{nr}$ increased by more than 1 order of magnitude upon warming the solution at room temperature. In EtOH and CF_3CH_2OH, at 298 K, the lifetime was slightly longer and the sum of the nonradiative rate constants was slightly smaller than in 3MP.

Among the radiationless processes involved in the relaxation dynamics of FL, there is the reactive route. Figure 2 shows the time evolution of the FL absorption spectrum recordable under continuous UV irradiation, due to the photoproduction of a yellowish species that is metastable, since it thermally back converts to FL (eq 1).[8]

$$\mathrm{FL} \underset{\Delta}{\overset{h\nu}{\rightleftharpoons}} \mathrm{B} \qquad (1)$$

The overall chemical transformation is described by the kinetic eq 2,

$$\frac{dA_B}{dt} = \epsilon_B I_{FL} \Phi_{PC} d - k_\Delta A_B \qquad (2)$$

where A_B and ϵ_B are the absorbance and the molar extinction coefficient of the product, respectively; I_{FL} represents the

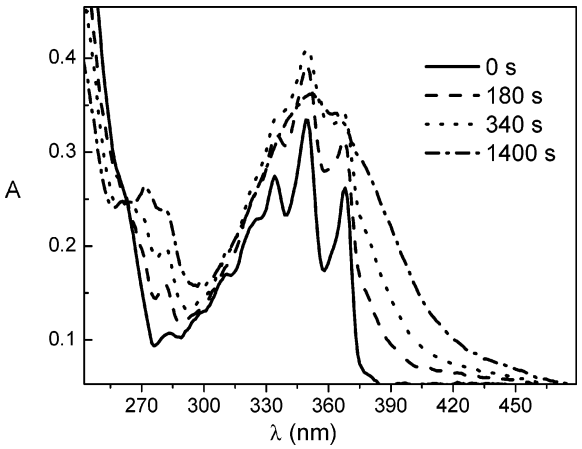

Figure 2. Spectral evolution of FL in 3MP upon continuous irradiation (λ_{exc} = 321 nm) at 150 K.

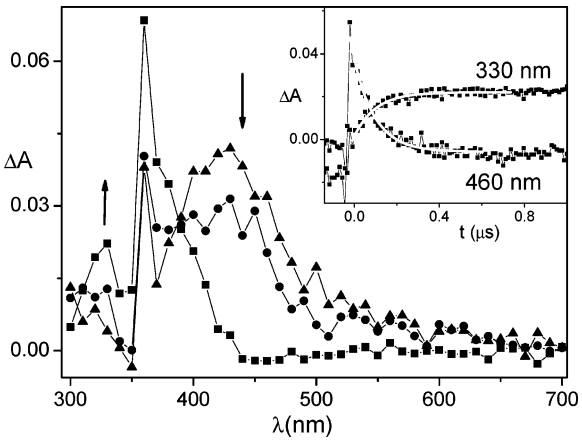

Figure 3. Transient absorption spectra of FL recorded in 3MP, at different delay times after the laser shot (λ = 355 nm): after 0.016 μs (triangle); after 0.052 μs (circle); and after 1.66 μs (square). Inset: Kinetics at 330 and 460 nm.

intensity of the irradiating monochromatic light (321 nm) absorbed by FL; d is the path length; and k_Δ is the rate constant for the thermal back conversion of B to FL. By adopting the kinetic method of the initial rates, determining the irradiation intensity, and knowing that $\epsilon_B = 3110$ dm^3 mol^{-1} cm^{-1} at 385 nm,[8] Φ_{PC} could be determined at different temperatures, using eq 3,

$$\Phi_{PC} = \frac{(dA_B/dt)_{t\to 0}}{I^0[1 - \exp(-2.3A_{FL})]\epsilon_B} \qquad (3)$$

where I^0 is the intensity of the incident light (321 nm) and A_{FL} is the FL absorbance at λ_{exc}.

Determinations of Φ_{PC} carried out at 260, 225, 210, 195, 180, 150, and 83 K showed that Φ_{PC} is constant and equal to 0.81 over the 260−80 K temperature range. This means that the rate constant (k_{PC}) of FL electrocyclization does not depend on either temperature or viscosity (η), since, in the broad range of temperatures investigated, η changes by 4×10^{12} times.

Nanosecond laser flash photolysis experiments allowed the role played by the triplet state in the relaxation dynamics of FL to be characterized. The spectral evolution of FL in 3MP (λ_{exc} = 355 nm) is portrayed in Figure 3. Two transients are involved (as also found for 2,2-spiro-adamantyl-7,8-benzo(2*H*)chromene):[11] the first, appearing soon after the laser excitation, gives rise to the band centered at 430 nm and has a lifetime of 0.1 μs, which was shortened in the presence of oxygen; this transient

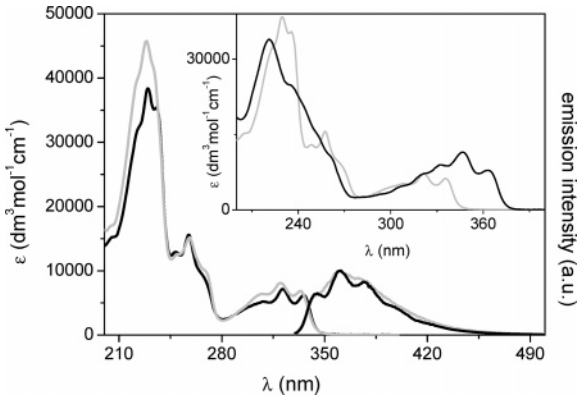

Figure 4. Absorption and emission spectra of PH in ethanol (black) and acetonitrile (gray) recorded at room temperature. Inset: Comparison of absorption spectra of FL (black) and PH (gray) in ethanol.

annihilates to produce, at least partially, the second component, whose spectrum has a maximum at 360 nm. This latter transient is insensitive to oxygen and has a lifetime in the millisecond scale. Its spectral and dynamical properties suggest that it is the product (B in eq 1) of the electrocyclization reaction. Its precursor can be reasonably thought to be a triplet state of FL. The triplet character of the precursor transient was supported by diffusional quenching by oxygen ($k_q = 2 \times 10^9$ dm^3 mol^{-1} s^{-1}), 2,2,6,6-tetramethyl-1-piperidinyl-1-oxy radical (TEMPO; $k_q = 4.6 \times 10^9$ dm^3 mol^{-1} s^{-1}), and ferrocene ($k_q = 2 \times 10^{10}$ dm^3 mol^{-1} s^{-1}). Moreover, FL quenched the room-temperature camphorquinone (E_T = 210 kJ mol^{-1})[18] phosphorescence emission ($k_q = 4 \times 10^8$ dm^3 mol^{-1} s^{-1}). As a consequence, sensitization experiments, carried out with the purpose of determining the triplet quantum yield of FL, were unsuccessful when biacetyl (E_T = 236 kJ mol^{-1})[15] was used as a triplet energy acceptor, whereas they were successful with β-carotene (E_T = 75 kJ mol^{-1}).[19] The product $\Phi_T \times \epsilon_T$ (where ϵ_T and Φ_T are the triplet absorption coefficient and quantum yield, respectively) was measured at 430 nm. By means of the procedure mentioned in the experimental section, the following values were obtained in benzene at 430 nm: $\Phi_T \times \epsilon_T = 2710$ dm^3 mol^{-1} cm^{-1}, $\Phi_T = 0.33$, and $\epsilon_T = 8210$ dm^3 mol^{-1} cm^{-1}. Therefore, the rate constant of $S_1 \rightarrow T_1$ intersystem crossing is $k_{ISC}(298K) = \Phi_T/\tau_F \approx 2 \times 10^9$ s^{-1}.

The triplet state lifetime was reduced to almost one-half in polar solvents: resulting in 0.055 μs in ethanol. When FL was excited at 266 nm, the same spectral evolution as that at 355 nm was obtained.

6(5*H*)-Phenanthridinone (PH). The 6(5*H*)-phenanthridinone (PH) is a heterocyclic compound, whose molecular structure is strictly related to that of the photochromic FL (see Chart 1). Consequently, the absorption spectra of PH and FL are very similar, Figure 4, inset. Similar to FL, even for PH, the band at lower energy is vibronically structured with an average energy separation between adjacent peaks of 1400 cm^{-1}. This kind of fine structure can also be found in the fluorescence spectrum centered at 360 nm (see Figure 4).

The magnitude of the molar absorption coefficients (10^4 dm^3 mol^{-1} cm^{-1}) of the spectrum of PH points to allowed electronic transitions, as in FL. ZINDO/S (10 × 10) calculation, performed on a geometry optimized for the electronic ground state with the PM3 method, predicts a band at 312 nm, having π,π^* nature and involving a π system delocalized over the entire phenanthrene-type framework containing the amide group. Moreover, a n,π^* state, associated with the carbonyl group, is predicted to originate a forbidden transition at 340 nm.

TABLE 3: Stokes Shift and Fluorescence Quantum Yield (Φ_F) Determined for PH in Various Solvents, with or without Oxygen, at Room Temperature and for Different Excitation Wavelengths

solvent	Stokes shift/$\Delta\bar{\nu}$ (cm^{-1})	λ_{exc} (nm)	Φ_F(aerated)	Φ_F(deaerated)
3MP	528	320 (S_1)	0.064	0.066
		269 (S_2)	0.046	0.047
		255 (S_2)	0.044	0.045
		225 (S_3)	0.041	0.042
CH_3CN	870	319 (S_1)	0.068	0.071
		267 (S_2)	0.059	0.061
		258 (S_2)	0.053	0.055
EtOH	648	319 (S_1)	0.106	0.108
		267 (S_2)	0.106	0.108
		258 (S_2)	0.091	0.092
		234 (S_3)	0.074	0.075
H_2O	1032	320 (S_1)	0.128	0.130
		256 (S_2)	0.082	0.084
		230 (S_3)	0.078	0.081
CF_3CH_2OH	954	320 (S_1)	0.13	0.14
		293 (S_1)	0.13	0.14
		255 (S_2)	0.11	0.12

Different from FL, PH exhibited a solubility strongly dependent on the solvent: it was scarcely soluble in saturated and unsaturated hydrocarbons, as well as in water, whereas it easily dissolved in solvents like ethanol and acetonitrile.

Fluorescence quantum yields, determined in air equilibrated and nitrogen equilibrated solutions, Table 3, reveal that some photophysical properties of PH, like Stokes shift and Φ_F, are significantly sensitive to the nature of the solvent. In particular, increasing polarity and/or hydrogen bonding ability of the solvent leads to an increase in both Φ_F and Stokes shift, as found for FL. Moreover, the Φ_F value in each solvent was independent of the degree of vibronic excitation within the same electronic transition, but decreased passing from excitation in the lowest energy electronic band to excitation in the higher ones. This occurred, albeit PH was unreactive under UV irradiation during the recording of emission spectra. The fluorescence quantum yield of PH was also sensitive to temperature, as it occurred in FL. A sevenfold increase was observed in 3MP between room temperature ($\Phi_F = 0.044$) and 80 K ($\Phi_F = 0.31$), a temperature where phosphorescence also was observed ($\Phi_P = 0.41$). In ethanol, Φ_F increased $^5/_2$ times from 333 ($\Phi_F = 0.093$) to 174 K ($\Phi_F = 0.232$), whereas it rose of almost 2 times from 328 ($\Phi_F = 0.114$) to 245 K ($\Phi_F = 0.202$) in trifluoroethanol.

By using the single photon counting method and the hydrogen lamp as the exciting source, τ_F of PH was also determined in different solvents and at different temperatures. In Figure 5, the experimental τ_F and Φ_F values are plotted as a function of temperature in 3MP (a) and ethanol (b). Both Φ_F and τ_F increased by lowering the temperature and their growth occurs with substantially the same slope. This suggests that the radiative rate constant, k_F, is quite independent of temperature.

In Table 4, τ_F, k_F, and $\sum k_{nr}$, determined at 298 K in three solvents, are reported. The fluorescence lifetime increased by raising the polarity and/or proticity of the solvent. This is mainly due to a decrease of the nonradiative kinetic constants, whose sum is the most temperature-sensitive parameter, whereas k_F, which was substantially the same in the three solvents, is independent of temperature.

At 80 K, in a 3MP matrix, PH gave rise to a phosphorescence band besides the fluorescence one, confirming what was reported in ref 20. From the spectral position of the phosphorescence band the triplet state energy, $E_T = 285$ kJ mol^{-1}, was estimated. Through nanosecond flash photolysis experiments the spectral

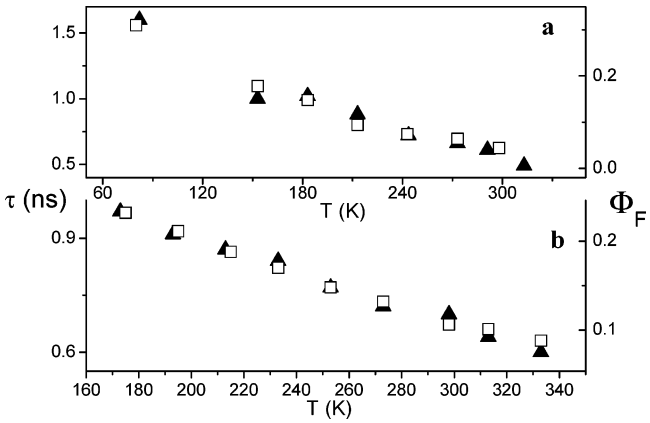

Figure 5. Variation with temperature of fluorescence quantum yield (Φ_F, right side scale) and lifetime (τ_F, left side scale) of PH in 3MP (a) and ethanol (b). The fluorescence decay traces were collected at $\lambda_{exc} = 320$ nm and $\lambda_{em} = 357$ nm.

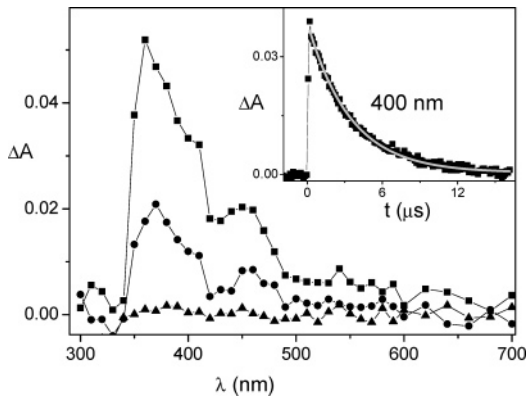

Figure 6. Transient absorption spectra of PH recorded in acetonitrile at room temperature, at different delay times after the laser shot (λ = 266 nm): after 0.56 μs (square); after 4.16 μs (circle); and after 15.3 μs (triangle). Inset: kinetics at 400 nm.

TABLE 4: Fluorescence Lifetimes and Radiative and Nonradiative Kinetic Constants of PH in Trimethylpentane, Ethanol, and Trifluoroethanol

solvent	T/K	τ_F/ns	k_F/s^{-1}	$\sum k_{nr}/s^{-1}$
3MP	78	1.6	1.9×10^8	4.3×10^8
	298	0.6	1.1×10^8	1.6×10^9
EtOH	298	0.7	1.6×10^8	1.3×10^9
	173	0.97	2.3×10^8	8×10^8
CF_3CH_2OH	298	0.92	1.4×10^8	9.5×10^8

and kinetic properties of the triplet state were determined. The transient absorption spectra, collected soon after the laser pulse ($\lambda_{exc} = 266$ nm), involved only one transient species, originating a broadband, peaked at 360 nm (Figure 6). This species exhibited triplet character since it was quenched by oxygen, sensitized by benzophenone, and decayed with monoexponential kinetics ($\tau = 3.3$ μs, in deaerated acetonitrile solution, Figure 6, inset).

By using benzophenone ($E_T = 288$ kJ mol^{-1}) as a triplet sensitizer, the molar absorption coefficient of PH was determined ($\epsilon_T = 6000 \pm 400$ dm^3 mol^{-1} cm^{-1} at 400 nm, and $\epsilon_T = 8500 \pm 500$ dm^3 mol^{-1} cm^{-1} at 370 nm). From $\Phi_T \times \epsilon_T$ values at the different wavelengths, the triplet quantum yield, $\Phi_T = 0.8 \pm 0.1$ in CH_3CN, was obtained. Through measurements of biacetyl sensitized phosphorescence (see the Experimental Section) carried out in ethanol at room temperature, with 2,2′-dithienylketone as a reference, the triplet quantum yield was estimated to be $\Phi_T = 0.74 \pm 0.1$. It is worth noticing that Φ_T is substantially the same in both solvents, ethanol and

TABLE 5: Fluorescence Quantum Yields of Thioxanthone, Phenanthridine, and Acridine as a Function of the Excitation Wavelength, in Ethanol at Room Temperature

thioxanthone		phenanthridine		acridine	
λ_{exc} (nm)	Φ_F	λ_{exc} (nm)	Φ_F	λ_{exc} (nm)	Φ_F
377	0.072	329	0.111	374	0.022
297	0.050	298	0.082	355	0.019
285	0.050	288	0.075	338	0.016
		269	0.069	258	0.007

acetonitrile, with respect to the accuracy with which it could be determined. Since the lifetime of PH is $\tau = 0.7$ ns in ethanol at room temperature, $k_{ISC} \approx 1 \times 10^9$ s^{-1}.

Further Results. We wanted to ascertain whether the fluorescence quantum yield dependence on excitation of different electronic bands was a peculiarity of PH and FL or if it was detectable even in other compounds already known to give "proximity effects" in their photophysics. For this purpose, we recorded the emission, absorption, and emission excitation spectra of thioxanthone,[21] phenanthridine,[22] and acridine[23] in ethanol at room temperature and determined the fluorescence quantum yields as a function of λ_{exc} (Table 5). As found for FL and PH, Φ_F decreased by passing from excitation at the lowest energy electronic band to excitation at higher energy bands also for thioxanthone, phenanthridine, and acridine.

Discussion

The close structural similarity between FL and PH entails related energetic distribution of the electronic excited states and therefore similar absorption and emission spectra. It is reasonable to suppose that the two heterocyclic compounds also have similar relaxation dynamics after UV irradiation. However, the presence of a pyran ring, exclusively in FL, opens the possibility of an electrocyclization reactive path, that is so fast as to kinetically compete with the other decay routes.[11] The consequence is that all quantum yields of radiative and radiationless processes, other than chemical transformation, are smaller for FL than for PH. The latter is more luminescent than FL, has a higher Φ_T than FL, and exhibits phosphorescence emission in a 3MP matrix at 80 K. Moreover, the lifetimes of the excited singlet and triplet states are shorter for FL than for PH. Since both FL and PH have an amide group in their antenna systems, both compounds are expected to have two close-lying electronic excited states of n,π^* and π,π^* nature. This implies the possible detection of "proximity effects" in their photophysics, namely, luminescence sensitive to the proticity of the solvent and temperature.

The fluorescence quantum yields and decay lifetimes of FL and PH depend on the nature of the solvent. In nonpolar solvents, fluorescence is weak and short lived. It becomes more intense and longer lived by increasing the proticity of the solvent. The hydrogen-bonding power of solvent molecules can modify the n,$\pi^*-\pi,\pi^*$ energy gap, shifting the n,π^* state to the blue and the π,π^* state to the red. If the lowest excited state is π,π^* in character the n,$\pi^*-\pi,\pi^*$ energy gap increases in protic solvents, thus reducing the n,$\pi^*-\pi,\pi^*$ vibronic coupling and leading to an intensity and lifetime increase of the luminescence, as observed for both PH and FL. Hydrogen-bonding interaction is favored by formation of a stable six-member cycle involving the amide group of the compound and the OH group of the solvent (Chart 2).

The temperature is the other parameter able to control the vibronic coupling between the n,$\pi^*-\pi,\pi^*$ states and modulate the luminescence from S_1. Considering the possibility of a thermally activated radiationless process, the total nonradiative rate constant $\sum k_{nr}$ can be separated into a temperature-independent part $\sum(k'_{nr})$ and a temperature-dependent part (eq 4),[24]

CHART 2

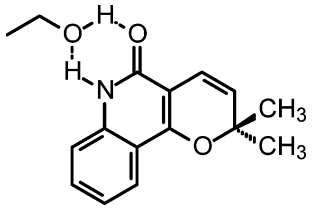

TABLE 6: Activation Energies and Frequency Factors of PH and FL in Trimethylpentane, Ethanol, and Trifluoroethanol

	PH		FL	
solvent	E_a (cm^{-1})	A (s^{-1})	E_a (cm^{-1})	A (s^{-1})
3MP	420 ± 20	2×10^{10}	475 ± 14	1×10^{11}
EtOH	580 ± 50	2×10^{10}	880 ± 50	5×10^{11}
CF_3CH_2OH	940 ± 50	5×10^{10}	1360 ± 130	10^{12}

$$\sum k_{nr} = \sum (k'_{nr}) + A e^{-E_a/RT} \quad (4)$$

where A is the frequency factor and E_a is the activation energy. Insertion of eq 4 into the expression of fluorescence quantum yield results in the Arrhenius-type eq 5:

$$\frac{1}{\Phi_F} = \frac{k_F + \sum k'_{nr}}{k_F} + \frac{A}{k_F} e^{-E_a/RT} = \frac{1}{\Phi_F^0} + \frac{A}{k_F} e^{-E_a/RT} \quad (5)$$

where k_F is the fluorescence kinetic constant. In logarithmic form, eq 5 becomes:

$$\ln\left(\frac{1}{\Phi_F} - \frac{1}{\Phi_F^0}\right) = \ln\left(\frac{A}{k_F}\right) - \frac{E_a}{RT} \quad (6)$$

where $\Phi_F^0 = (k_F)/(k_F + \sum k'_{nr})$ represents the low-temperature limit of Φ_F.

A similar equation can be formulated for the fluorescence lifetime

$$\ln\left(\frac{1}{\tau_F} - \frac{1}{\tau_F^0}\right) = \ln(A) - \frac{E_a}{RT} \quad (7)$$

where $\tau_F^0 = 1/(k_F + \sum k'_{nr})$ represents the low-temperature limit of τ_F.

The analysis of the Φ_F and τ_F data by relationships 6 and 7 (see a graphical example for PH in 3MP, Figure 7) allows the activation energies and the frequency factors for FL and PH to be determined. The results obtained in solvents of different proticity are reported in Table 6. It is evident that the activation energies are quite small for both compounds, confirming a close proximity of the (n,π^*) and (π,π^*) states. As expected, the E_a values significantly increase by raising the solvent proticity. Even the frequency factors are solvent dependent: they increase along with the hydrogen-bonding power of the solvent and their values for FL are roughly 10 times greater than those determined for PH. The magnitude of the frequency factors suggests that a spin-allowed process[24] is the principal temperature-dependent decay route. This is underpinned by a theoretical consideration, predicting the proximity effect to be greater the larger the energy

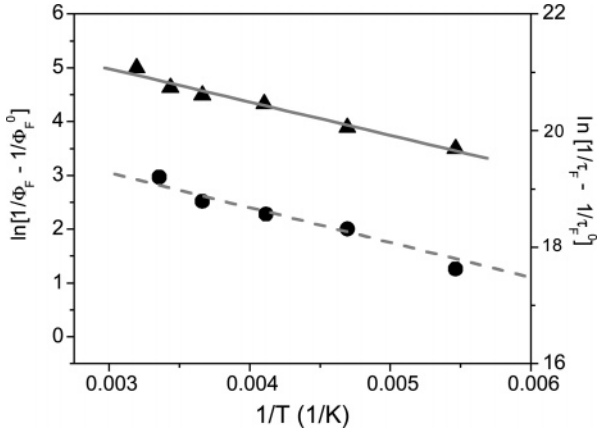

Figure 7. Temperature dependence of fluorescence quantum yield (circle) and lifetime (triangle) of PH in 3MP according to eqs 6 and 7, respectively.

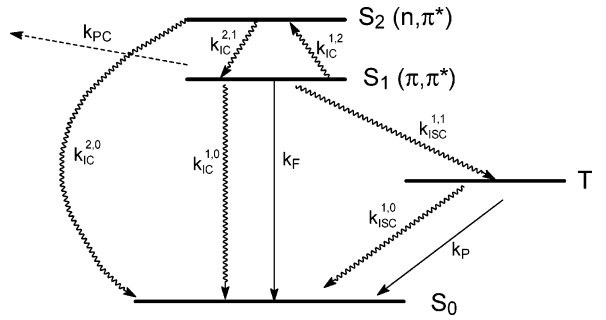

Figure 8. Energy level diagram and kinetic scheme of the relaxation dynamics for the lowest singlet excited states of FL and PH.

gap for a radiationless transition is.[25] Since the S_1-S_0 energy gap is much greater than the S_1-T_1 gap, it follows that the proximity effect should have a much larger effect on $S_1 \rightarrow S_0$ internal conversion than on $S_1 \rightarrow T_1$ intersystem crossing.

Due to the remarkably small energy gap between S_2 (n,π*) and S_1 (π,π*) states, a strong coupling is predictable for them. As reported by Siebrand and Zgierski,[2] under strong coupling conditions, higher order contributions to radiationless decay must be considered, namely, transitions in which the upper of the two coupled states acts as an intermediate. On the basis of this consideration, the kinetic model that we propose to explain the obtained results is portrayed in Figure 8. It includes, among the relaxation pathways that can be pursued from the $S_1(\pi,\pi^*)$ state, not only fluorescence decay, intersystem crossing to triplet state, and internal conversion directly to S_0 ($k_{IC}^{1,0}$), but also an activated internal conversion to a slightly higher singlet excited state S_2 (n,π*) ($k_{IC}^{1,2}$). In FL there is also the temperature-independent electrocyclization reactive branch (k_{PC}) to take into account. As the S_2 state is populated, it is depleted through either internal conversion to S_1 ($k_{IC}^{2,1}$) or directly to S_0 ($k_{IC}^{2,0}$), bypassing S_1. On the basis of this scheme, already proposed in a similar fashion to explain the isoquinoline photophysics,[26] the fluorescence quantum yield is related to the rate constants through eq 8:

$$\frac{1}{\Phi_F} = \frac{k_F + k_{IC}^{1,0} + k_{ISC} + (k_{PC})}{k_F} + \frac{k_{IC}^{2,0} A_{1,2} e^{-E_a^{1,2}/RT}}{(k_{IC}^{2,0} + k_{IC}^{2,1}) k_F} \quad (8)$$

The experimentally determined frequency factor (A) of eq 5 can be identified with the ratio $(k_{IC}^{2,0}A_{1,2})/(k_{IC}^{2,0} + k_{IC}^{2,1})$ of eq 8. Therefore,

$$A_{1,2} = A\left(1 + \frac{k_{IC}^{2,1}}{k_{IC}^{2,0}}\right) \quad (9)$$

From eq 9, it is clear-cut that $A_{1,2} \geq A$, namely, $A_{1,2} \geq 10^{11}-10^{12}$ s^{-1} in FL, whereas $A_{1,2} \geq (2-5) \times 10^{10}$ s^{-1} in PH. Since S_2 is close in energy to S_1, it is reasonable that $k_{IC}^{2,1}$ is comparable with $A_{1,2}$. Therefore, to deplete S_1 significantly, $k_{IC}^{2,0}$ must be $\geq(2-5) \times 10^{10}$ s^{-1} in PH and $k_{IC}^{2,0} \geq 10^{11}-10^{12}$ s^{-1} in FL. The internal conversion $S_2 \rightarrow S_0$ should be the main route which, by subtracting population to S_1, is responsible for the dependence of the fluorescence quantum yield on temperature and excitation wavelength. If electronic states located at higher energy than the lowest n,π* and π,π* ones are excited, a fraction of molecules can undertake the route that bypasses S_1, reducing the quantum yield of fluorescence. This is probably true not only for FL and PH, but also for other N-heterocyclics and carbonyl compounds, such as thioxanthone, phenanthridine, and acridine, which exhibit proximity effects.

Conclusions

This work highlights the role played by the carbonyl group in the antenna system of a naturally occurring chromene, FL, and the structurally related heterocyclic compound, PH. The carbonyl group entails the existence of two close-lying n,π* and π,π* electronic states, whose energy can be modulated through a careful choice of the hydrogen-bonding power of the solvent. In a nonprotic solvent, like 3MP, n,π* and π,π* states are very close, whereas in the highly protic trifluoroethanol, they can be far apart. The closer the energy of the n,π* and π,π* states, the stronger their coupling is. The temperature is the other parameter whereby it is possible to control the coupling of the two states: the two orthogonal electronic states can couple through out-of-plane bending vibrations of the carbonyl group. The higher the temperature, the larger is the energy available to the coupling modes. More energy to these modes entails stronger coupling between the two electronic excited states. The stronger their coupling, the faster the radiationless decay and the lower the Φ_F are. In FL the emissive power is further reduced with respect to PH by the very fast reactive route, able to kinetically compete with the other relaxation branches.[8]

As theoretically predicted by Siebrand and Zgierski,[2] and previously proposed by Turro et al. for the *all-trans*-retinal,[27] the strong coupling between n,π* and π,π* states can also be the cause of the dependence on the degree of electronic excitation of Φ_F. FL and PH, as thioxanthone, phenanthridine, acridine, *all-trans*-retinal, and probably other *N*-heterocyclic and carbonyl compounds, exhibit a decrease in Φ_F when optically active electronic states, located at energies greater than those of the n,π* and π,π* states, are selectively excited. This phenomenology can be accounted for by the ability to subtract molecules from the emissive $S_1(\pi,\pi^*)$ level of the dark n,π* state, which can be populated from either higher states or thermally from $S_1(\pi,\pi^*)$. In fact, under strong coupling conditions, contributions to radiationless decay by transitions, in which the upper of the two coupled states acts as an intermediate, must be considered. By this way a decay route is opened which bypasses S_1, reducing the emission.

Acknowledgment. This research was funded by the Italian "Ministero per l'Università e la Ricerca Scientifica e Tecnologica" and the University of Perugia in the framework of a FIRB project (Spectroscopic and kinetic study of organic photochromic compounds in solution, micro-heterogeneous media and polymeric films).

References and Notes

(1) Lim, E. C. *J. Phys. Chem.* **1986**, *90*, 6770−6777 and references therein.

(2) Siebrand, W.; Zgierski, M. Z. *J. Chem. Phys.* **1981**, *75*, 1230−1238 and an earlier paper of this series.

(3) Hanawa, F.; Fokialakis, N.; Skaltsounis, A. L. *Planta Med.* **2004**, *70* (6), 531−535.

(4) (a) Braz-Filho, R. *Pure Appl. Chem.* **1999**, *71* (9), 1663−1672. (b) Malquichagua Salazar, K. J.; Delgado Paredes, G. E.; Lluncor, L. R.; Max Young, M. C.; Kato, M. J. *Phytochemistry* **2005**, *66*, 573−579.

(5) Van Gemert, B. In *Organic Photochromic and Thermochromic Compounds*; Crano J. C., Guglielmetti, R. J., Eds.; Plenum Press: New York, 1999; Vol. 1 and references therein.

(6) Migani, A.; Gentili, P. L.; Negri, F.; Olivucci, M.; Romani, A.; Favaro, G.; Becker, R. S. *J. Phys. Chem. A* **2005**, *109*, 8684−8692.

(7) Becker, R. S.; Dolan, E.; Balke, D. E. *J. Chem. Phys.* **1969**, *50*, 239−245.

(8) Becker, R. S.; Pelliccioli, A. P.; Romani, A.; Favaro, G. *J. Am. Chem. Soc.* **1999**, *121*, 2104−2109.

(9) Favaro, G.; Romani, A.; Becker, R. S. *Photochem. Photobiol.* **2001**, *74*, 378−384.

(10) (a) Becker, R. S.; Favaro, G.; Romani, A.; Gentili, P. L.; Dias, F. M. B. *Chem. Phys.* **2005**, *316*, 108−116. (b) Gentili, P. L.; Romani, A.; Becker, R. S.; Favaro, G. *Chem. Phys.* **2005**, *309*, 167−175.

(11) Gentili, P. L.; Danilov, E.; Rodgers, M. A.; Ortica, F.; Favaro, G. *Photochem. Photobiol. Sci.* **2004**, *3*, 886−891.

(12) Becker, R. S.; Favaro, G.; Poggi, G.; Romani, A. *J. Phys. Chem.* **1995**, *99*, 1410−1417.

(13) Melhuish, W. H. *J. Phys. Chem.* **1961**, *65*, 229−235.

(14) Mantulin, W. W.; Huber, J. R. *Photochem. Photobiol.* **1973**, *17*, 139−143.

(15) Murov, S. L.; Carmichael, I.; Hug, G. L. In *Handbook of Photochemistry*; Marcel Dekker Inc.: New York, 1993.

(16) Carmichael, I.; Hug, G. L. *J. Phys. Chem. Ref. Data* **1986**, *15*, 1−250.

(17) Kumar, C. V.; Qin, L.; Das, P. K. *J. Chem. Soc., Faraday Trans. 2* **1984**, *80*, 783−793.

(18) Romani, A.; Favaro, G.; Masetti, F. *J. Lumin.* **1995**, *63*, 183−188.

(19) Scaiano, J. C. In *Handbook of Organic Photochemistry*; CRC Press Inc.: Boca Raton, FL, 1989.

(20) Val'kova, G. A.; Sakhno, T. V.; Shcherbo, S. N.; Shigorin, D. N.; Andrievskii, A. M.; Poplavskii, A. N.; Dyumaev, K. M. *Russ. J. Phys. Chem.* **1980**, *54* (9), 1382−1383.

(21) (a) Lai, T.; Lim, E. C. *Chem. Phys. Lett.* **1980**, *73*, 244−248. (b) Lai, T.; Lim, E. C. *Chem. Phys. Lett.* **1981**, *84*, 303−307.

(22) Lim, E. C.; Yu, J. M. H. *J. Chem. Phys.* **1967**, *47*, 3270−3275.

(23) Madej, S. L.; Okajima, S.; Lim, E. C. *J. Chem. Phys.* **1976**, *65*, 1219−1220.

(24) Birks, J. B. In *Photophysics of aromatic molecules*; Wiley: London, UK, 1970.

(25) (a) Wassam, W. A., Jr.; Lim, E. C. *J. Chem. Phys.* **1978**, *68*, 433−454. (b) Wassam, W. A., Jr.; Lim, E. C. *J. Chem. Phys.* **1978**, *69*, 2175−2180.

(26) Huber, J. R.; Mahaney, M.; Morris, J. V. *Chem. Phys.* **1976**, *16*, 329−335.

(27) Turro, N. J.; Ramamurthy, V.; Cherry, W.; Farneth, W. *Chem. Rev.* **1978**, *78*, 125−145.